



Online-Appendix zu

„Measuring the Impact of MiFID II on Information Asymmetries Using Microstructure Models“

Erik-Jan Senn

Eberhard Karls Universität Tübingen

Junior Management Science 5(2) (2020) 197-208

7 Appendix

7.1 Derivations

Model assumptions (Madhavan et al.)

$$E(x) = 0 \quad (14)$$

$$P(x_t = x_{t-1} | x_{t-1} \neq 0) = \gamma \quad (15)$$

$$P(x = 0) = \lambda \quad (16)$$

$$P(x_t = -x_{t-1} | x_{t-1} \neq 0) = 1 - \gamma - \lambda \quad (17)$$

The Madhavan et al. model assumptions are necessary for the calculation of the price change and the model implied spreads. Eq. (14) states that the mean for the trade indicator is assumed to be 0. Eq. (15) defines the probability γ of a transaction at the bid (ask) following a transaction at the bid (ask) and is expected to be greater than 0.5. The unconditional probability of a trade inside the spread is defined in Eq. (16) as λ . The probability for a trade at the bid (ask) following a trade at the ask (bid) in Eq. (17) follows from Eq. (15) and (16).

Derivation 1: Autocorrelation of order flow ρ (Madhavan et al.)

$$\rho_t = \frac{E[(x_t - E(x_t))(x_{t-1} - E(x_{t-1}))]}{\sigma_{x_t} \sigma_{x_{t-1}}}$$

$$\rho = \frac{E(x_t x_{t-1})}{\sigma_x^2}$$

$$\sigma_x^2 = P(x = 1)(1)^2 + P(x = -1)(-1)^2 + P(x = 0)(0)$$

$$= 1 - \lambda$$

$$E(x_t x_{t-1}) = P(x_{t-1} \neq 0) P(x_t = x_{t-1} | x_{t-1} \neq 0)(1)$$

$$+ P(x_{t-1} \neq 0) P(x_t = -x_{t-1} | x_{t-1} \neq 0)(-1)$$

$$+ P(x_{t-1} \neq 0) P(x_t = 0 | x_{t-1} \neq 0)(0)$$

$$+ P(x_{t-1} = 0)(0)$$

$$= (1 - \lambda)\gamma - (1 - \lambda)(1 - \gamma - \lambda)$$

$$= (1 - \lambda)(2\gamma - (1 - \lambda))$$

$$\rho = 2\gamma - (1 - \lambda)$$

The general definition of the first-order autocorrelation is given in the first line. With $E(x_t) = 0$ (see Eq. (14)) and $\sigma_{x_t} \sigma_{x_{t-1}} = \sigma_x^2$ (weak stationarity assumption), the first-order autocorrelation only depends on the constant variance σ_x^2 and $E(x_t x_{t-1})$. The probabilities in Eq. (16), (15) and (17) lead to $E(x_t x_{t-1})$, which is then divided by $(1 - \lambda)$ to obtain ρ .

Derivation 2: Conditional expected trade indicator $E(x_t|x_{t-1})$ (Madhavan et al.)

$$\begin{aligned}
E(x_t|x_{t-1} = 1) &= P(x_t = 1|x_{t-1} = 1)(1) \\
&\quad + P(x_t = -1|x_{t-1} = 1)(-1) \\
&\quad + P(x_t = 0|x_{t-1} = 1)(0) \\
&= \gamma - (1 - \gamma - \lambda) \\
&= \rho
\end{aligned}$$

$$\begin{aligned}
E(x_t|x_{t-1} = -1) &= P(x_t = 1|x_{t-1} = -1)(1) \\
&\quad + P(x_t = -1|x_{t-1} = -1)(-1) \\
&\quad + P(x_t = 0|x_{t-1} = -1)(0) \\
&= (1 - \gamma - \lambda) - \gamma \\
&= -\rho
\end{aligned}$$

$$E(x_t|x_{t-1} = 0) = 0$$

$$E(x_t|x_{t-1}) = \rho x_{t-1}$$

The conditional expected trade indicator $E(x_t|x_{t-1})$ can be expressed by the first-order autocorrelation ρ . With Eq. (14) and $\rho = 2\gamma - (1 - \lambda)$ from derivation 1, the expected trade indicator given the 3 different cases of x_{t-1} simplifies to ρ , $-\rho$ and 0.

Derivation 3: Price change ΔP_t (Madhavan et al.)

$$\begin{aligned}
P_t &= \mu_{t-1} + \theta(x_t - E(x_t|x_{t-1})) + \phi x_t + u_t \\
\Delta P_t &= \mu_{t-1} + \theta(x_t - E(x_t|x_{t-1})) + \phi x_t + u_t \\
&\quad - (\mu_{t-2} + \theta(x_t - E(x_{t-1}|x_{t-2})) + \phi x_{t-1} + u_{t-1}) \\
&= \mu_{t-1} + \theta(x_t - E(x_t|x_{t-1})) + \phi x_t + u_t - \mu_{t-1} - \phi x_{t-1} \\
&= \theta(x_t - x_{t-1}\rho) + \phi x_t - \phi x_{t-1} + u_t \\
&= (\phi + \theta)x_t - (\phi + \rho\theta)x_{t-1} + u_t
\end{aligned}$$

The post-trade expected fundamental value in Eq. (1) is combined with the transitory component in Eq. (3) to form the transaction price P_t . When taking differences, the fundamental value is canceled out. With $E(x_t|x_{t-1}) = \rho x_{t-1}$ (see Eq. (5)), the price change ΔP_t can be described with the 4 model parameters ϕ, θ, ρ and λ , which is included in ρ (see derivation 1).

Derivation 4: Realized spread s_R (Madhavan et al.)

$$\begin{aligned}
s_R &= |E[P_{t+k} - P_t]| \\
&= |E[(\mu_{t+k-1} + \theta(x_{t+k} - E(x_{t+k}|x_{t+k-1})) + \phi x_{t+k} + u_{t+k}) - (\mu_t + \phi x_t)]| \\
&= |E[(\mu_{t+k-1} + (\theta + \phi)x_{t+k} + u_{t+k}) - (\mu_t + \phi x_t)]| \\
&= |E(\mu_{t+k-1}) - E(\mu_t) + E(u_{t+k}) + E[(\phi + \theta)x_{t+k} - \phi x_t]| \\
&= |E[(\phi + \theta)x_{t+k} - \phi x_t]| \\
&= (1 - \lambda)^2(2\phi + \theta) + \lambda(1 - \lambda)(\phi + \theta) + (1 - \lambda)\lambda\phi + \lambda^2(0) \\
&= (1 - \lambda)(2\phi + \theta) \\
s_R(x_t \neq 0) &= P(x_{t+k} \neq 0|x_t \neq 0)(2\phi + \theta) + P(x_{t+k} = 0|x_t \neq 0)\phi \\
&= (1 - \lambda)(2\phi + \theta) + \lambda\theta \\
s_R(x_t = 0) &= P(x_{t+k} \neq 0|x_t = 0)(\phi + \theta) + P(x_{t+k} = 0|x_t = 0)(0) \\
&= (1 - \lambda)(\phi + \theta)
\end{aligned}$$

The expected realized spread s_R is the cost of a buy (sell) in t and a sell (buy) in $t + k$ when ignoring the effect of autocorrelation (see Madhavan et al., 1997, p.1050). Using the price process in Eq. (3) with Eq. (1), $E(u_t) = 0$ and $E(\mu_{t+k-1}) = \mu_t$ under the assumption of no autocorrelation yields a simplified expression for the expected realized spread without the fundamental value. The four fundamentally different potential changes are from ask to bid, midquote to ask, ask to midquote and midquote to midquote (see Madhavan et al., 1997, p.1050). The probabilities for the paths $(1 - \lambda)^2$, $\lambda(1 - \lambda)$, $(1 - \lambda)\lambda$ and λ^2 and the corresponding cost $(2\phi + \theta)$, $(\phi + \theta)$, θ and zero lead to the expected realized spread s_E . The conditional realized spreads are calculated by only taking into account the possible paths based on the condition.

Derivation 5: Realized spread $s_{R,t}$ (Glosten-Harris)

$$\begin{aligned}
s_{R,t} &= |E[P_{t+k} - P_t]| \\
&= |E[(\mu_{t+k-1} + z_t x_{t+k} + c_t x_{t+k} + u_{t+k}) - (\mu_t + c_t x_t)]| \\
&= |E[(c_t + z_t)x_{t+k} - c_t x_t]| \\
&= (1 - \lambda)^2(2c_t + z_t) + \lambda(1 - \lambda)(c_t + z_t) + (1 - \lambda)\lambda c_t + \lambda^2(0) \\
&= (1 - \lambda)(2c_t + z_t) \\
s_{R,t}(x_t \neq 0) &= (1 - \lambda)(2c_t + z_t) + \lambda z_t \\
s_{R,t}(x_t = 0) &= (1 - \lambda)(c_t + z_t)
\end{aligned}$$

The Glosten and Harris (1988) realized spread derivation is similar to the realized Madhavan et al. (1997) spread in derivation 4. The cost for the paths $(2c_t + z_t)$, $(c_t + z_t)$, z_t and zero do not depend on the trade volume in $t + k$ because both parts of the round-trip use the same volume.

7.2 Tables

Table 4: Descriptive statistics (Oct. 2017 - Mar. 2018)

	<i>Mean</i>		Std.Dev.		Skewness		Excess kurtosis	
	before	after	before	after	before	after	before	after
P	71.504	72.194	2.497	3.262	- 0.054	-0.645	0.974	7.497
ΔP	-0.002	-0.017	3.477	4.048	3.732	-4.618	35.388	23.548
v	11.906	12.292	23.555	30.844	1.333	1.105	2.873	5.092
x	0.004	-0.008	0.020	0.018	0.904	0.708	0.414	0.236
$tr./day$	517.175	603.303	111.602	126.729	0.743	1.500	3.556	7.034
s_Q	8.057	7.721	11.543	9.414	4.205	1.725	40.793	5.920
s_E	1.321	1.390	5.792	5.972	4.209	-1.096	40.095	3.922
$r_{Q,MQ}$	11.809	11.015	13.976	8.041	4.248	1.666	40.823	4.851
$r_{E,MQ}$	1.912	1.899	6.999	4.721	4.313	-1.046	41.673	4.574

Note. This table presents the descriptive statistics for key variables from October 1st, 2017, to March 31st, 2018. The mean, standard deviation, skewness and excess kurtosis of the individual security distributions are reported before and after the implementation of MiFID II. The following variables are included: price P in Euro, price change between trades ΔP in cent, trade indicator x , quoted/effective spread s_Q/s_E in cent, volume per trade v in 1000 shares, transactions per day $tr./day$, relative quoted/effective spread $r_{Q,MQ}/r_{E,MQ}$ in basis points.

Table 5: Parameter estimates (Glosten-Harris, Dec. 2017 - Jan. 2018)

	<i>all securities</i>				<i>single securities - significant β_i</i>		
	$\overline{\hat{\beta}_i}$	$\overline{\hat{\sigma}_{\hat{\beta}_i}}$	$\hat{\sigma}_{\overline{\hat{\beta}_i}}$	P	$H_0 : \beta_i = 0$	$\beta_i \geq 0$	$\beta_i \leq 0$
c_0	0.7173	0.000046	0.0831	<0.01%	100%	0%	100%
c_1	0.0007	<0.000001	0.0002	0.10%	40%	4%	50%
$z_{0,0}$	0.3950	0.000147	0.0908	0.01%	68%	6%	68%
$z_{0,1}$	0.3213	0.000199	0.0874	0.06%	68%	12%	62%
$z_{1,0}$	-0.0032	<0.000001	0.0007	<0.01%	58%	68%	4%
$z_{1,1}$	-0.0003	<0.000001	0.0005	57.25%	34%	22%	12%

Note. The table presents summary statistics of the Glosten-Harris model parameters estimates based on data from December 1st, 2017, to January 31st, 2018. The mean of estimated parameters $\overline{\hat{\beta}_i}$ and the mean of estimated parameter standard deviations $\overline{\hat{\sigma}_{\hat{\beta}_i}}$ are given with i denoting the individual securities. The estimated standard deviation of the mean estimated parameter $\hat{\sigma}_{\overline{\hat{\beta}_i}}$ is used to compute the p-value for the two-sided t-test on $\overline{\hat{\beta}_i}$. On a single security level, the share of significant parameters for two-sided and one-sided tests on a 5% level is provided. The parameter mean and standard deviation for c_0 , $z_{0,1}$ and $z_{0,1}$ are denoted in cent, the volume-dependent c_1 , $z_{1,0}$ and $z_{1,1}$ in cent per 100 shares.

Table 6: Spread estimates (Glosten-Harris, Dec. 2017 - Jan. 2018)

	<i>Mean</i>		<i>Std.Dev.</i>		<i>Paired t-Test</i>
	before	after	before	after	P
s_Q	2.006	2.586	2.079	2.384	0.03%
$r_{Q,Data}$	26.271	37.132	11.240	10.374	<0.01%
s_E	1.284	1.596	1.294	1.528	0.18%
$r_{E,Data}$	92.324	111.409	26.664	23.179	<0.01%
r_{Adv}	12.623	36.874	31.861	15.710	<0.01%

Note. This table presents model-implied estimated Glosten-Harris spreads and spread ratios before and after the implementation of MiFID II from December 1st, 2017, to January 31st, 2018. The mean $\overline{\hat{s}_i} / \overline{\hat{r}_i}$ and the estimator of the variance across the sample $\hat{\sigma}_{\overline{\hat{s}_i}} / \hat{\sigma}_{\overline{\hat{r}_i}}$ are reported in cents for the quoted spread s_Q and the effective spread s_E . The shares of implied to observed spread $r_{Q,Data}$ and $r_{E,Data}$ and the share of implied spread attributable to adverse selection r_{Adv} are denoted in percent. P-values for the paired t-test on difference in means before and after the MiFID II implementation are given in percent.

Table 7: Parameter estimates (Madhavan et al., Oct. 2017 - Mar. 2018)

	<i>all securities</i>				<i>single securities - significant β_i</i>		
	$\overline{\hat{\beta}_i}$	$\overline{\hat{\sigma}_{\hat{\beta}_i}}$	$\hat{\sigma}_{\overline{\hat{\beta}_i}}$	P	$H_0 : \beta_i = 0$	$\beta_i \geq 0$	$\beta_i \leq 0$
ρ	0.1100	0.000024	0.0028	<0.01%	100%	0%	100%
λ	0.3976	0.000007	0.0036	<0.01%	100%	0%	100%
ϕ	0.6069	0.000012	0.0692	<0.01%	100%	0%	100%
θ_0	0.3310	0.000041	0.0832	0.02%	80%	6%	76%
θ_1	0.4385	0.000066	0.0855	<0.01%	86%	4%	86%
α	-0.0035	0.000006	0.0034	31.62%	12%	18%	4%

Note. The table presents summary statistics of the Madhavan et al. model parameters estimates based on data from October 1st, 2017, to March 31st, 2018. The mean of estimated parameters $\overline{\hat{\beta}_i}$ and the mean of estimated parameter standard deviations $\overline{\hat{\sigma}_{\hat{\beta}_i}}$ are given with i denoting the individual securities. The estimated standard deviation of the mean estimated parameter $\hat{\sigma}_{\overline{\hat{\beta}_i}}$ is used to compute the p-value for the two-sided t-test on $\overline{\hat{\beta}_i}$. On a single security level, the share of significant parameters for two-sided and one-sided tests on a 5% level is provided. The parameter mean and standard deviation for ϕ , θ_0 , θ_1 and α are denoted in cent.

Table 8: Parameter estimates (Glosten-Harris, Oct. 2017 - Mar. 2018)

	<i>all securities</i>				<i>single securities - significant β_i</i>		
	$\overline{\hat{\beta}_i}$	$\overline{\hat{\sigma}_{\hat{\beta}_i}}$	$\hat{\sigma}_{\overline{\hat{\beta}_i}}$	P	$H_0 : \beta_i = 0$	$\beta_i \geq 0$	$\beta_i \leq 0$
c_0	0.6583	0.000014	0.0781	<0.01%	100%	0%	100%
c_1	0.0005	<0.000001	0.0001	<0.01%	60%	0%	66%
$z_{0,0}$	0.3460	0.000047	0.0733	<0.01%	76%	4%	78%
$z_{0,1}$	0.4653	0.000065	0.0933	<0.01%	86%	4%	82%
$z_{1,0}$	-0.0020	<0.000001	0.0005	0.05%	80%	80%	6%
$z_{1,1}$	-0.0008	<0.000001	0.0004	9.23%	44%	40%	12%

Note. The table presents summary statistics of the Glosten-Harris model parameters estimates based on data from October 1st, 2017, to March 31st, 2018. The mean of estimated parameters $\overline{\hat{\beta}_i}$ and the mean of estimated parameter standard deviations $\overline{\hat{\sigma}_{\hat{\beta}_i}}$ are given with i denoting the individual securities. The estimated standard deviation of the mean estimated parameter $\hat{\sigma}_{\overline{\hat{\beta}_i}}$ is used to compute the p-value for the two-sided t-test on $\overline{\hat{\beta}_i}$. On a single security level, the share of significant parameters for two-sided and one-sided tests on a 5% level is provided. The parameter mean and standard deviation for c_0 , $z_{0,1}$ and $z_{0,1}$ are displayed in cent, the volume-dependent c_1 , $z_{1,0}$ and $z_{1,1}$ in cent per 100 shares.

Table 9: Spread estimates (Madhavan et al., Oct. 2017 - Mar. 2018)

	<i>Mean</i>		<i>Std.Dev.</i>		Paired t-Test
	before	after	before	after	P
s_Q	1.876	2.753	1.920	2.446	<0.01%
$r_{Q,Data}$	25.237	36.599	10.677	9.806	<0.01%
s_E	1.140	1.649	1.134	1.515	<0.01%
$r_{E,Data}$	84.341	118.576	23.949	20.967	<0.01%
r_{Adv}	25.761	52.228	20.889	12.083	<0.01%

Note. This table presents model-implied estimated Madhavan et al. spreads and spread ratios before and after the implementation of MiFID II from October 1st, 2017, to March 31st, 2018. The mean $\widehat{s}_i / \widehat{r}_i$ and the estimator of the variance across the sample $\widehat{\sigma}_{\widehat{s}_i} / \widehat{\sigma}_{\widehat{r}_i}$ are reported in cents for the quoted spread s_Q and the effective spread s_E . The shares of implied to observed spread $r_{Q,Data}$ and $r_{E,Data}$ and the share of implied spread attributable to adverse selection r_{Adv} are denoted in percent. P-values for the paired t-test on difference in means before and after the MiFID II implementation are given in percent.

Table 10: Spread estimates (Glosten-Harris, Oct. 2017 - Mar. 2018)

	<i>Mean</i>		<i>Std.Dev.</i>		Paired t-Test
	before	after	before	after	P
s_Q	1.858	2.710	1.918	2.407	<0.01%
$r_{Q,Data}$	25.029	36.012	10.601	9.584	<0.01%
s_E	1.155	1.669	1.146	1.534	<0.01%
$r_{E,Data}$	85.549	119.935	24.112	21.304	<0.01%
r_{Adv}	16.670	46.138	21.773	10.869	<0.01%

Note. This table presents model-implied estimated Glosten-Harris spreads and spread ratios before and after the implementation of MiFID II from October 1st, 2017, to March 31st, 2018. The mean $\widehat{s}_i / \widehat{r}_i$ and the estimator of the variance across the sample $\widehat{\sigma}_{\widehat{s}_i} / \widehat{\sigma}_{\widehat{r}_i}$ are reported in cents for the quoted spread s_Q and the effective spread s_E . The shares of implied to observed spread $r_{Q,Data}$ and $r_{E,Data}$ and the share of implied spread attributable to adverse selection r_{Adv} are denoted in percent. P-values for the paired t-test on difference in means before and after the MiFID II implementation are given in percent.

7.3 Graphics

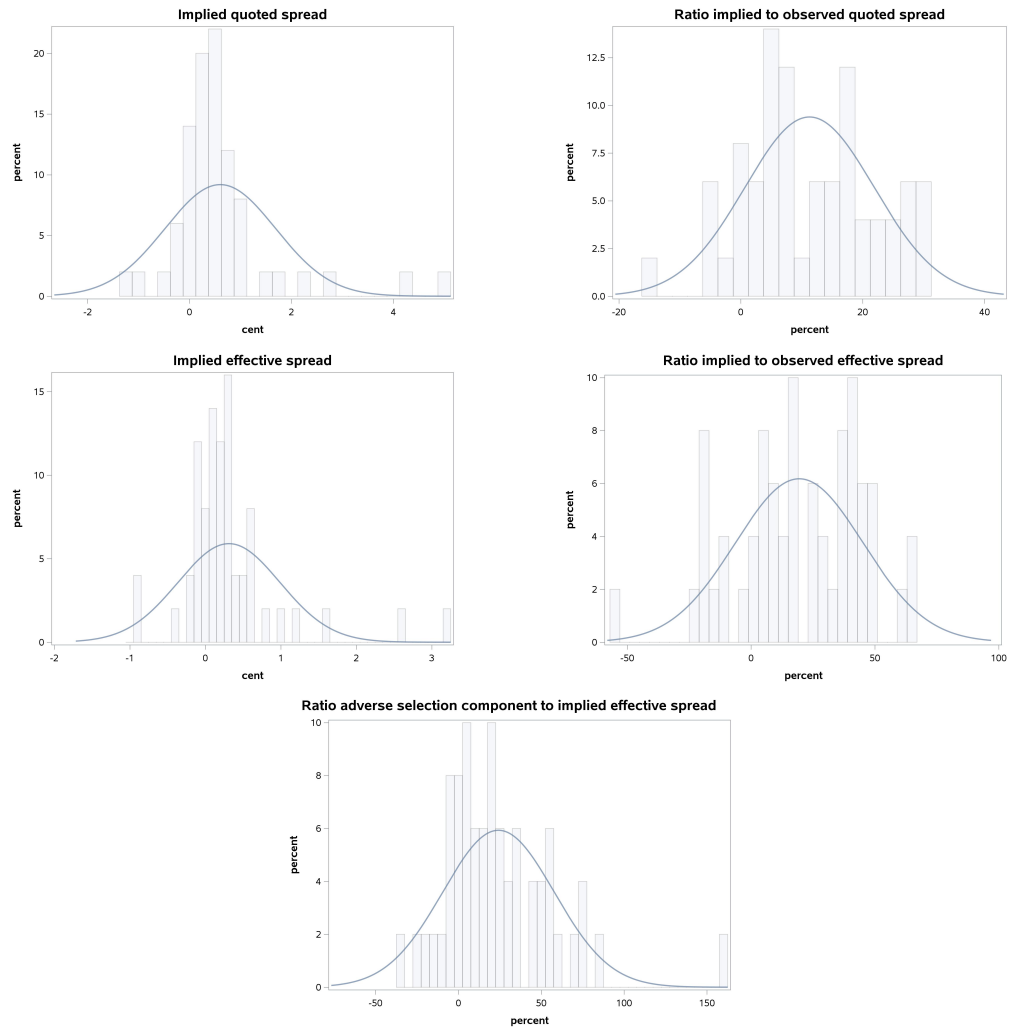


Figure 3: Difference distribution of estimated spread means (Madhavan et al., Dec. 2017 - Jan. 2018)
Note. These figures show the distribution of the individual security differences in mean for the following variables: implied quoted spread s_Q , share of implied quoted to observed quoted spread $r_{Q,Data}$, implied effective spread s_E , share of implied effective to observed effective spread $r_{E,Data}$ and share of implied spread attributable to adverse selection $r_{Adv,E}$. The assumption of normally distributed differences is necessary for the paired t-test and might be violated since most differences display a higher kurtosis than the normal distribution.

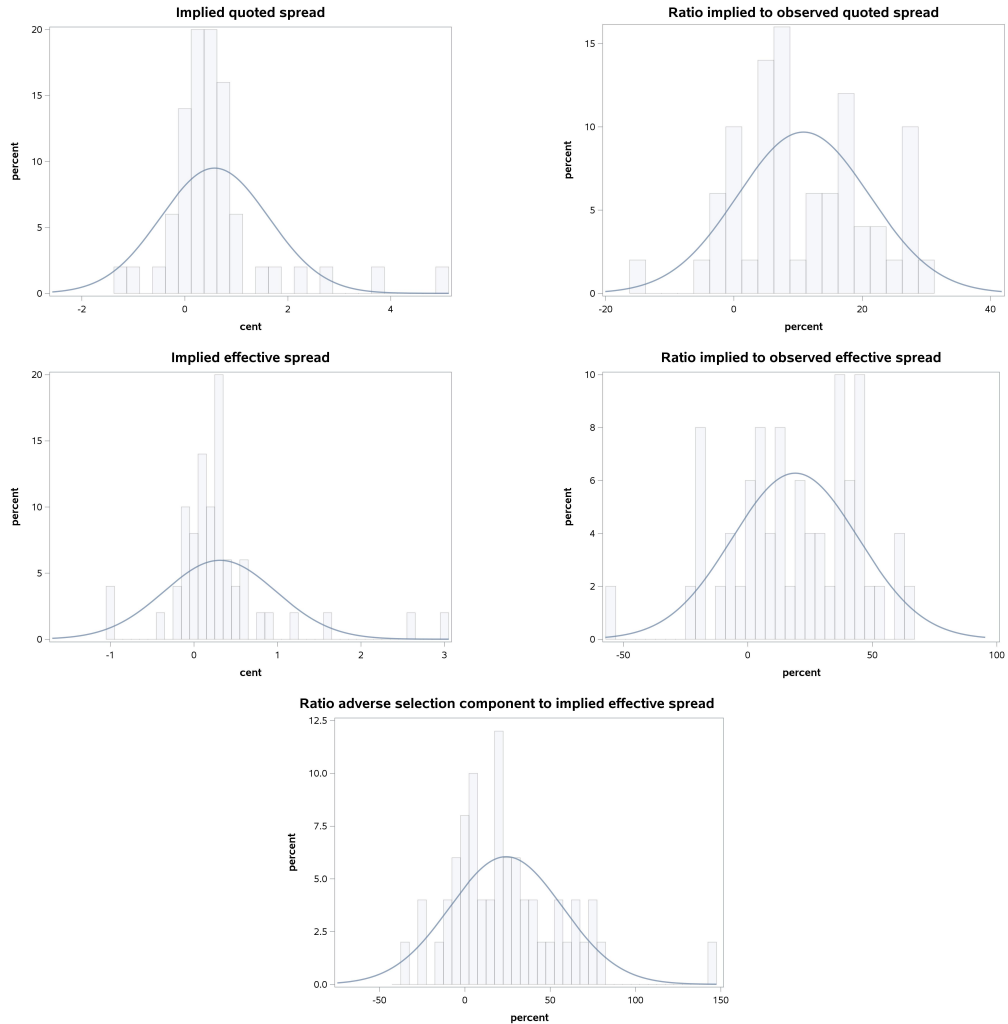


Figure 4: Difference distribution of estimated spread means (Glosten-Harris, Dec. 2017 - Jan. 2018)
Note. These figures show the distribution of the individual security differences in mean for the following variables: implied quoted spread s_Q , share of implied quoted to observed quoted spread $r_{Q,Data}$, implied effective spread s_E , share of implied effective to observed effective spread $r_{E,Data}$ and the share of implied spread attributable to adverse selection $r_{Adv,E}$. The assumption of normally distributed differences is necessary for the paired t-test and might be violated since most differences display a higher kurtosis than the normal distribution.

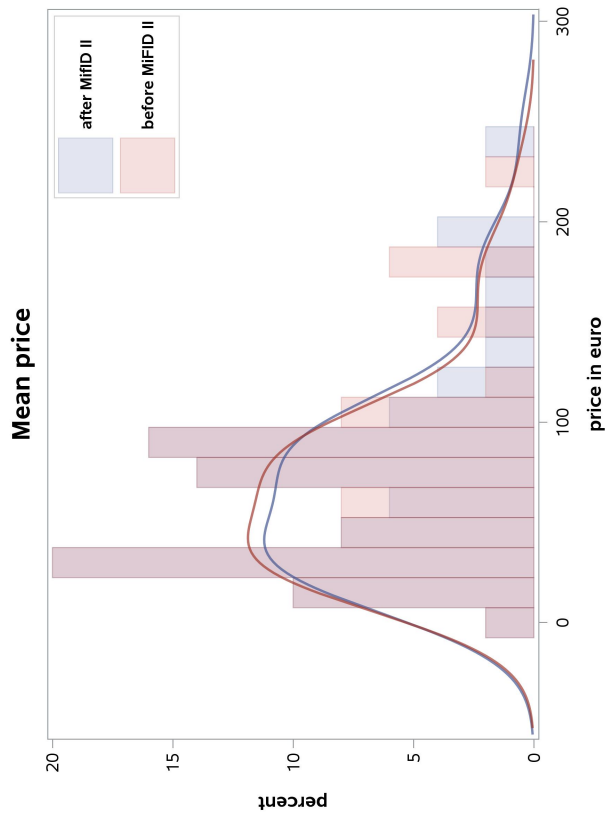


Figure 5: Histogram of prices

Note. This histogram shows the distribution of mean security prices from December 1st, 2017, to January 31st, 2018. The kernel density curve and bars are colored red for the distribution before and blue for the distribution after the implementation of MiFID II.

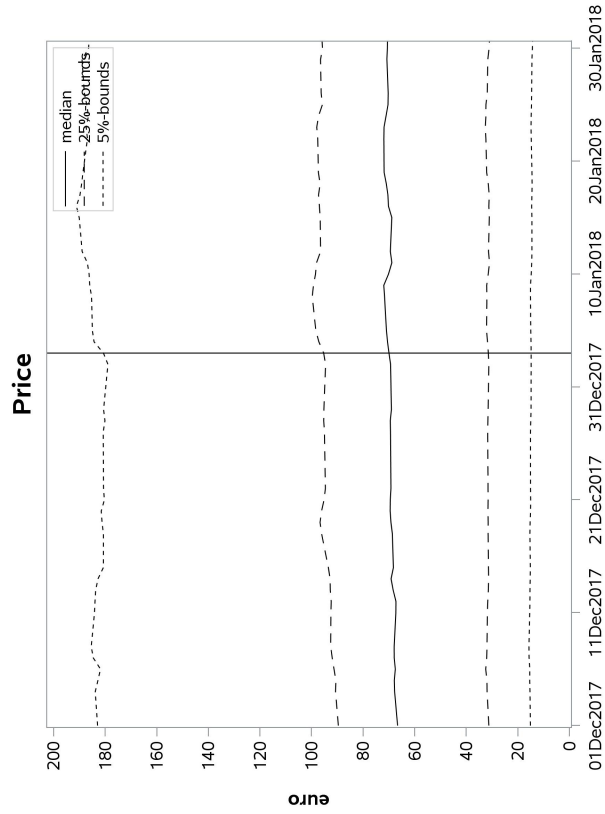


Figure 6: Time series of prices

Note. This figure shows the development and distribution of daily mean prices from December 1st, 2017, to January 31st, 2018. The vertical line displays the MiFID II implementation date.

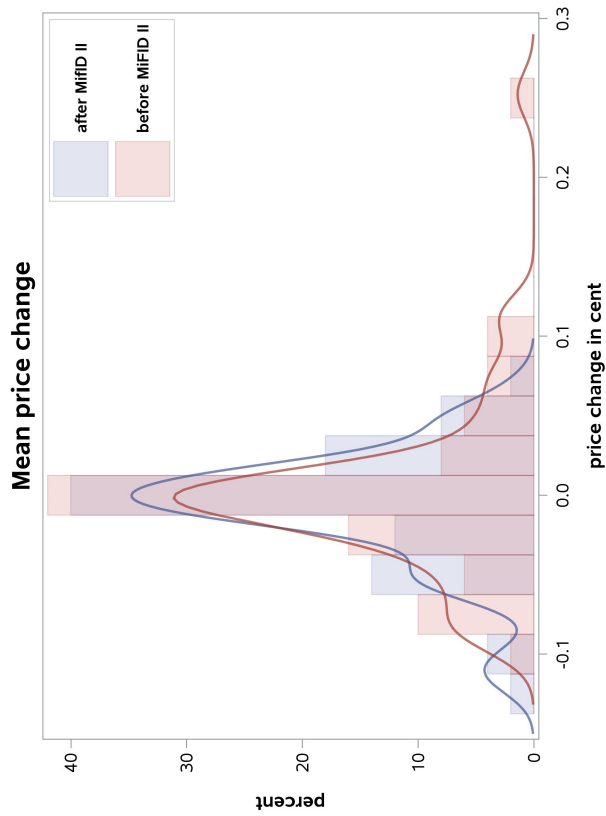


Figure 7: Histogram of price changes

Note. This histogram shows the distribution of mean security price changes from December 1st, 2017, to January 31st, 2018. The kernel density curve and bars are colored red for the distribution before and blue for the distribution after the implementation of MiFID II.

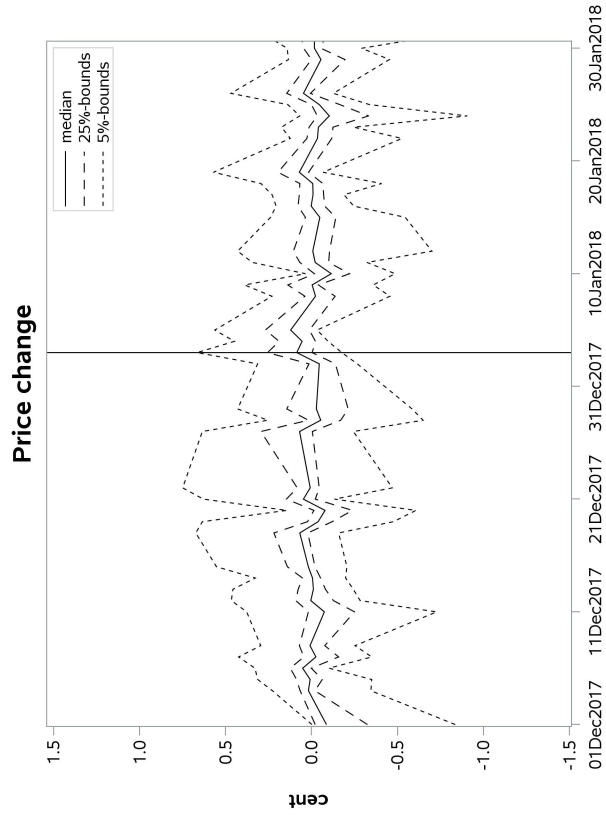


Figure 8: Time series of price changes

Note. This figure shows the development and distribution of daily mean price changes from December 1st, 2017, to January 31st, 2018. The vertical line displays the MiFID II implementation date.

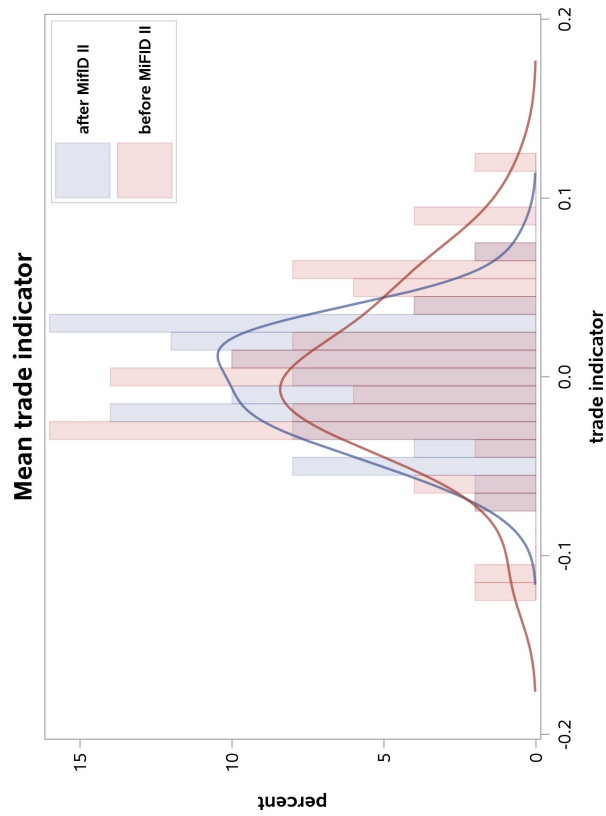


Figure 9: Histogram of trade indicators
Note. This histogram shows the distribution of mean trade indicators from December 1st, 2017, to January 31st, 2018. The kernel density curve and bars are colored red for the distribution before and blue for the distribution after the implementation of MiFID II. A value of 0 can be interpreted as equal number of buys and sells.

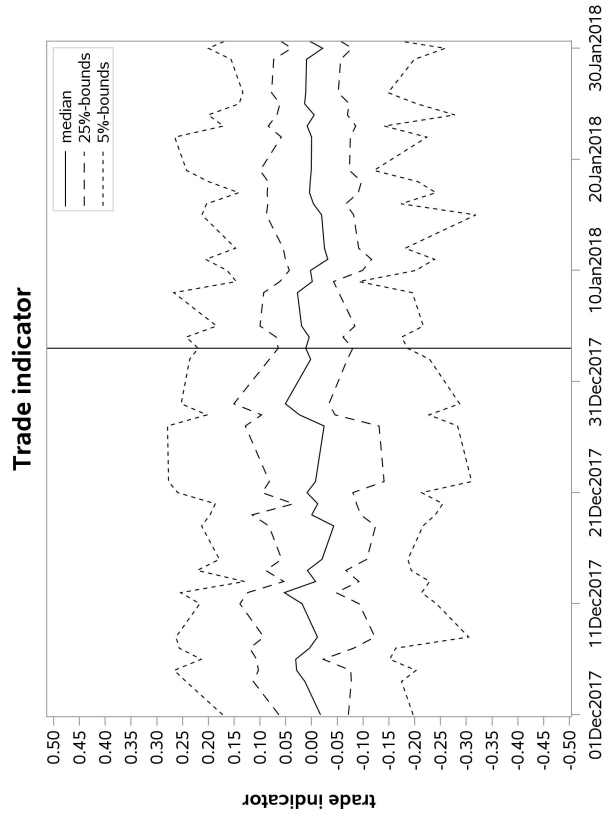


Figure 10: Time series of trade indicators
Note. This figure shows the development and distribution of daily mean trade indicators from December 1st, 2017, to January 31st, 2018. The vertical line displays the MiFID II implementation date.

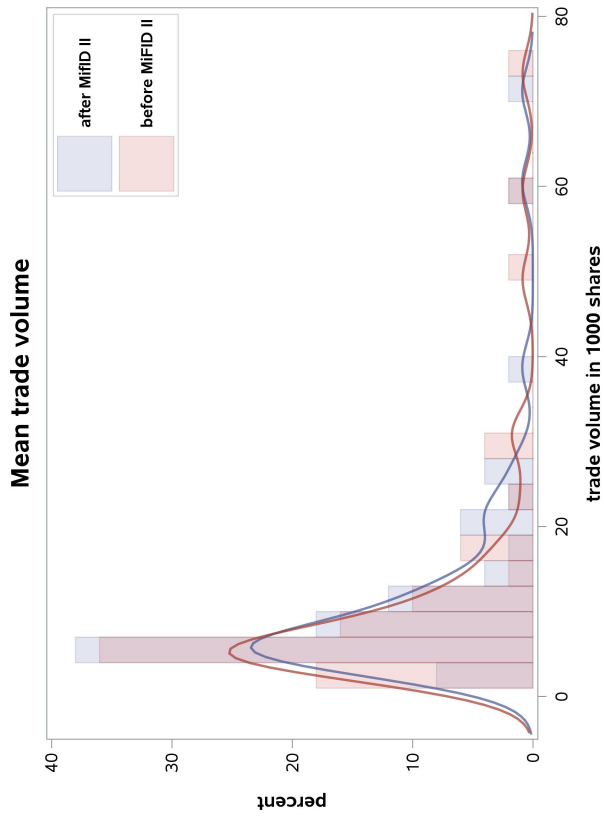


Figure 11: Histogram of trade volumes

Note. This histogram shows the distribution of mean trade volumes from December 1st, 2017, to January 31st, 2018. The kernel density curve and bars are colored red for the distribution before and blue for the distribution after the implementation of MiFID II. The skewness of trade volume is amplified by the trade aggregation process which adds up volumes of multiple trades in one second.

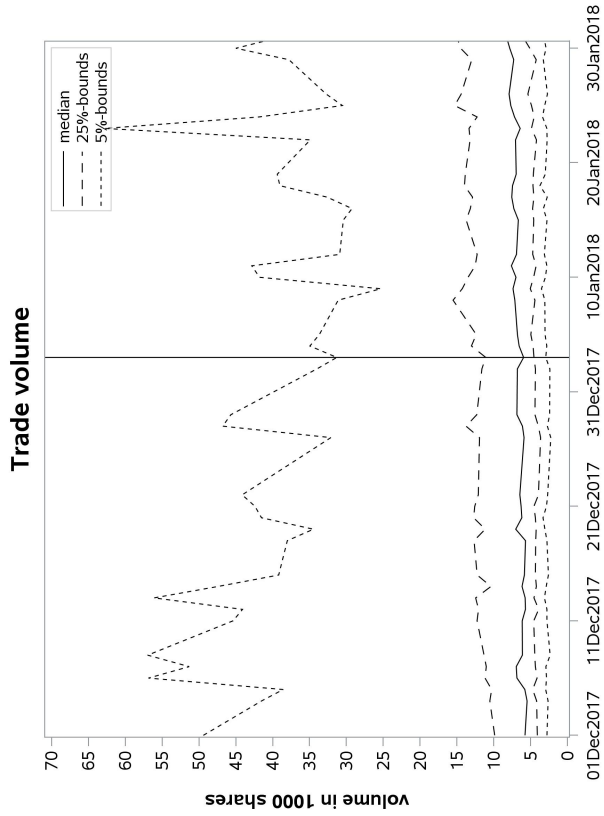


Figure 12: Time series of trade volumes

Note. This sideways figure shows the development and distribution of daily mean trade volumes from December 1st, 2017, to January 31st, 2018. The vertical line displays the MiFID II implementation date.

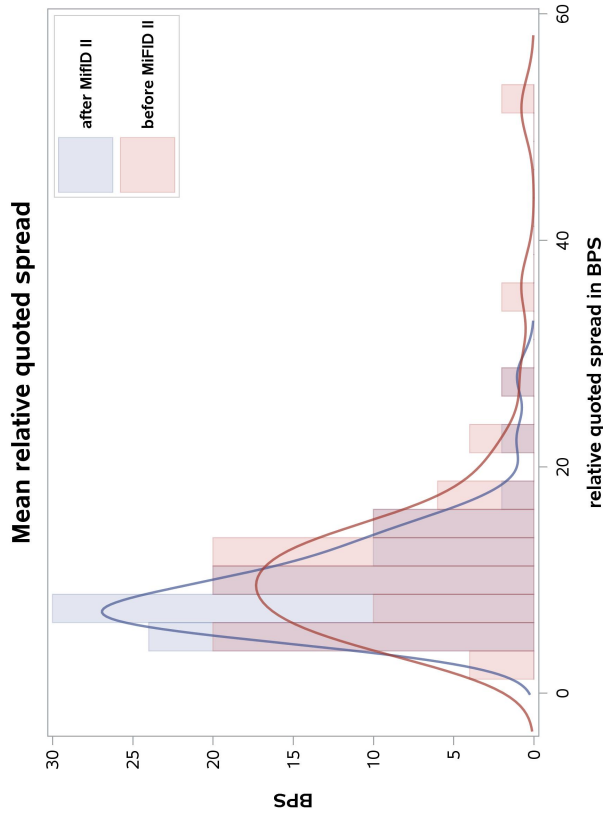


Figure 13: Histogram of relative quoted spreads
Note. This histogram shows the distribution of mean relative quoted spreads from December 1st, 2017, to January 31st, 2018. The kernel density curve and bars are colored red for the distribution before and blue for the distribution after the implementation of MiFID II.

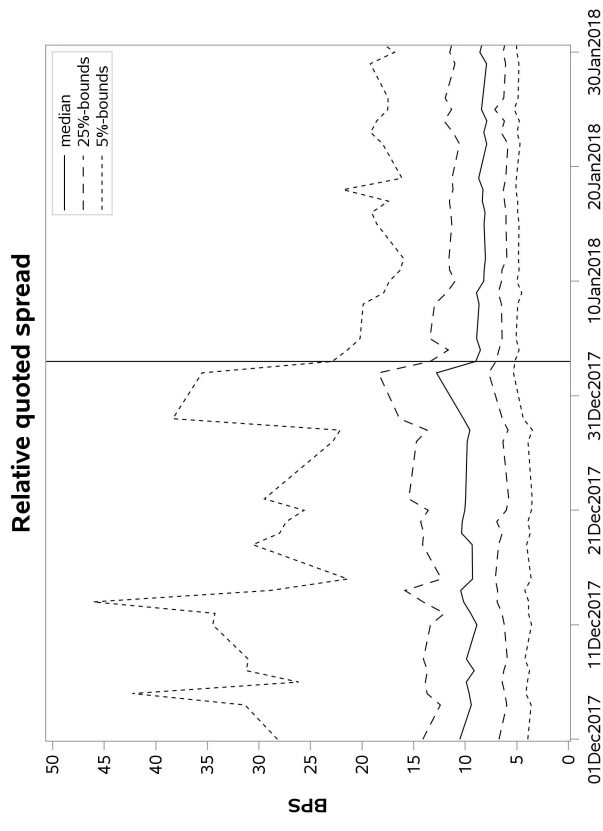


Figure 14: Time series of relative quoted spreads
Note. This sidewaysfigure shows the development and distribution of daily mean relative quoted spreads from December 1st, 2017, to January 31st, 2018. The vertical line displays the MiFID II implementation date.

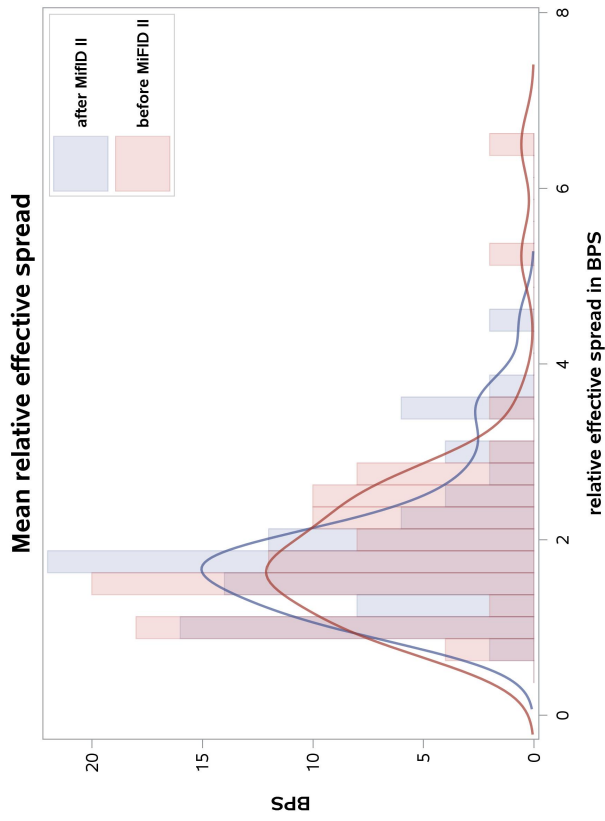


Figure 15: Histogram of relative effective spreads
Note. This histogram shows the distribution of mean relative effective spreads from December 1st, 2017, to January 31st, 2018. The kernel density curve and bars are colored red for the distribution before and blue for the distribution after the implementation of MiFID II.

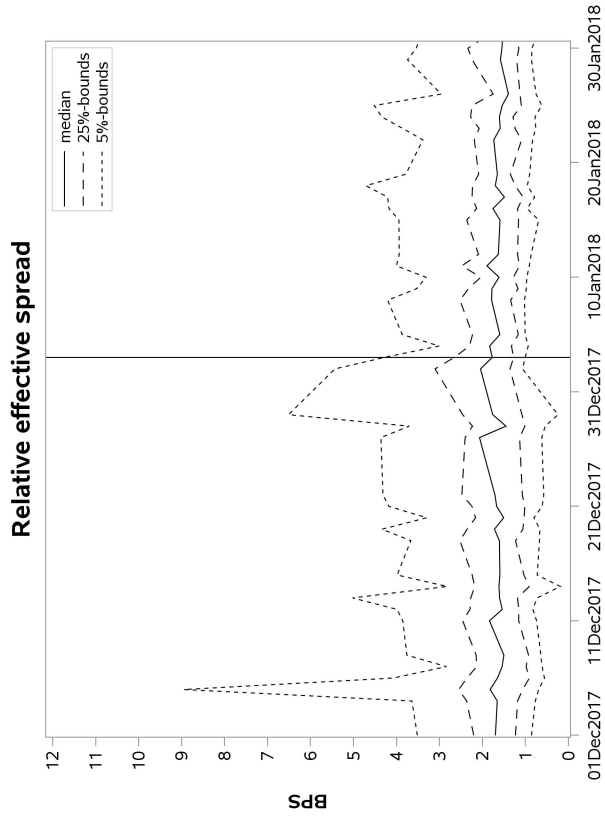


Figure 16: Time series of relative effective spreads
Note. This sidewaysfigure shows the development and distribution of daily mean relative effective spreads from December 1st, 2017, to January 31st, 2018. The vertical line displays the MiFID II implementation date.

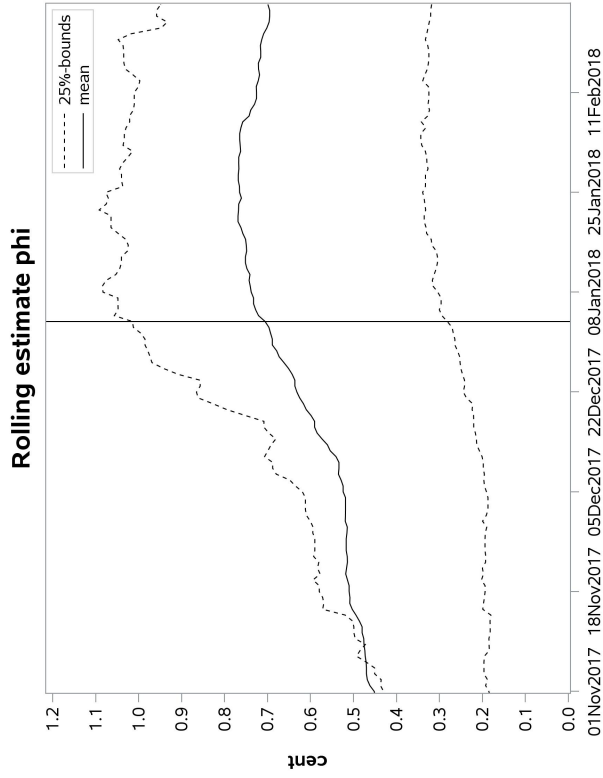


Figure 17: Rolling parameter estimate $\hat{\phi}$
Note. This figure plots the mean estimated Madhavan et al. parameter $\hat{\phi}$ for event dates from November to February with a two months estimation time frame. Starting from the event date, the additional adverse selection parameter is active. The vertical line displays the MiFID II implementation date.

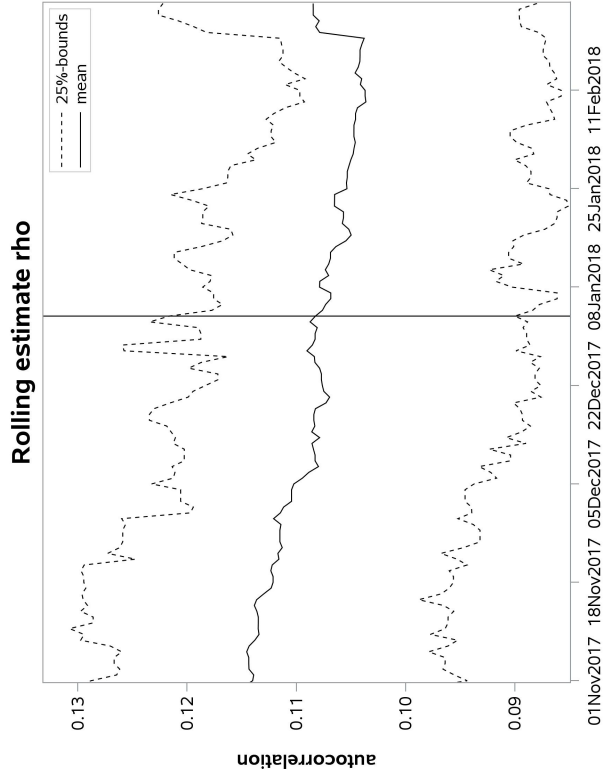


Figure 18: Rolling parameter estimate $\hat{\rho}$
Note. This figure plots the mean estimated Madhavan et al. parameter $\hat{\rho}$ for event dates from November to February with a two months estimation time frame. Starting from the event date, the additional adverse selection parameter is active. The vertical line displays the MiFID II implementation date.

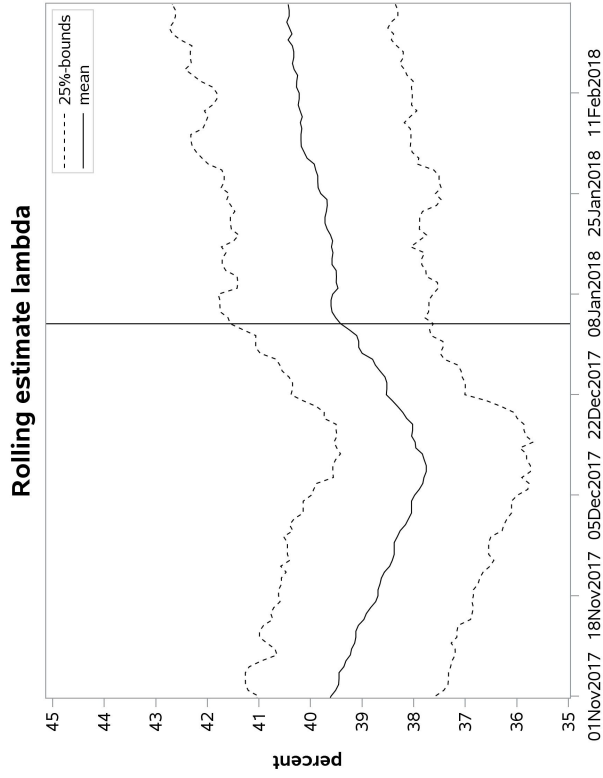


Figure 19: Rolling parameter estimate $\hat{\lambda}$

Note. This figure plots the mean estimated Madhavan et al. parameter $\hat{\lambda}$ for event dates from November to February with a two months estimation time frame. Starting from the event date, the additional adverse selection parameter is active. The vertical line displays the MiFID II implementation date.

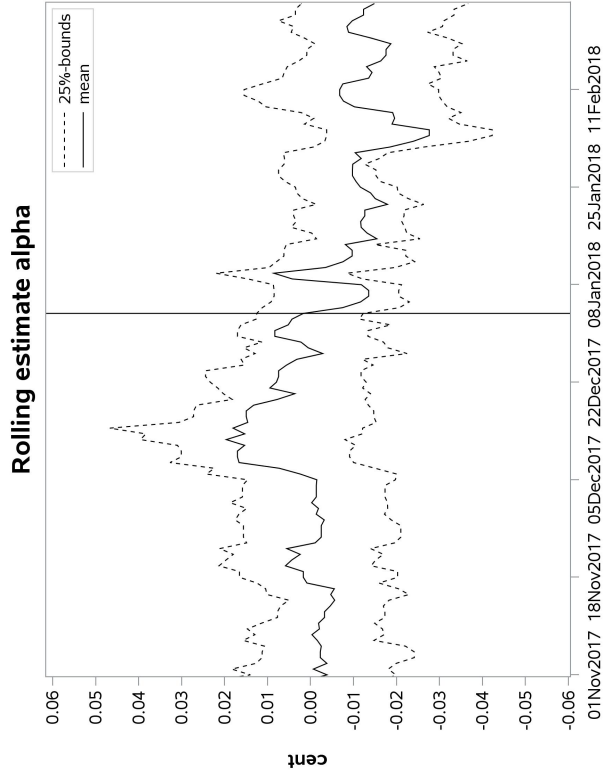


Figure 20: Rolling parameter estimate $\hat{\alpha}$

Note. This figure plots the mean estimated Madhavan et al. parameter $\hat{\alpha}$ for event dates from November to February with a two months estimation time frame. Starting from the event date, the additional adverse selection parameter is active. The vertical line displays the MiFID II implementation date.

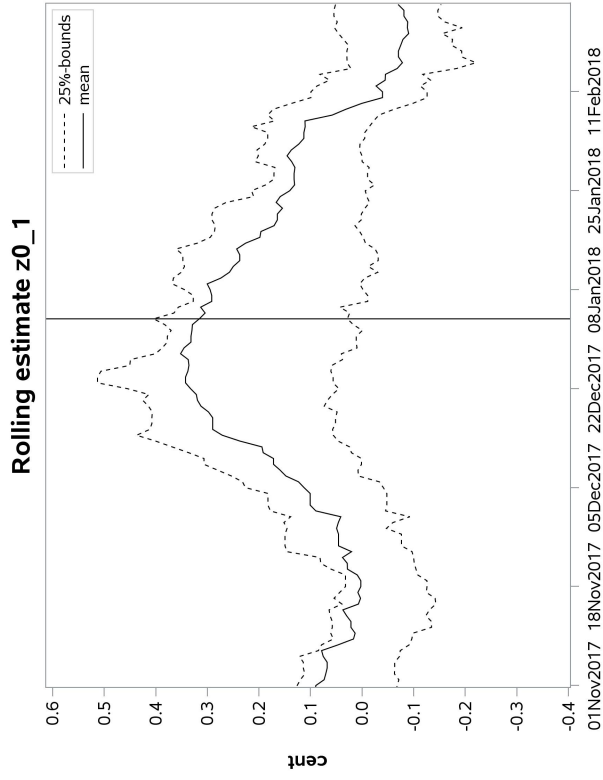


Figure 21: Rolling parameter estimate \hat{z}_{0_1}
Note. This figure plots the mean estimated Madhavan et al. parameter \hat{z}_{0_1} for event dates from November to February with a two months estimation time frame. Starting from the event date, the additional adverse selection parameters are active. The vertical line displays the MiFID II implementation date.

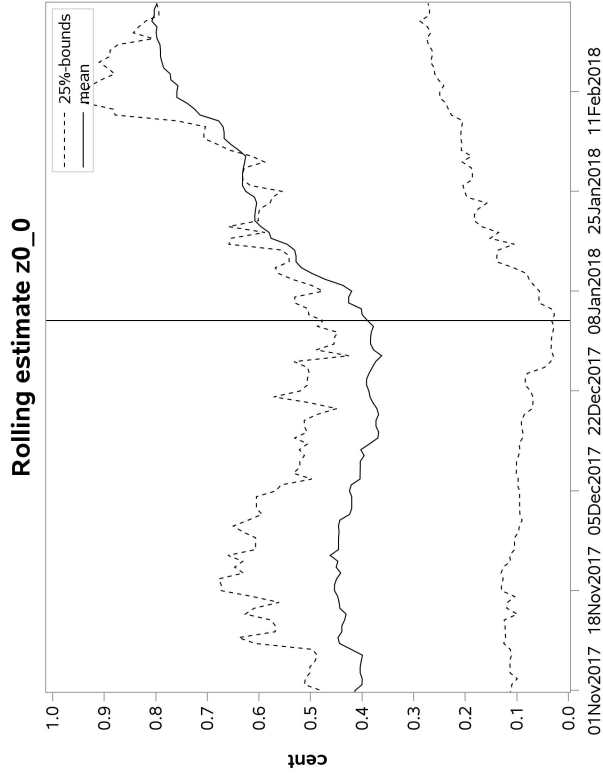


Figure 22: Rolling parameter estimate \hat{z}_{0_0}
Note. This figure plots the mean estimated Madhavan et al. parameter \hat{z}_{0_0} for event dates from November to February with a two months estimation time frame. Starting from the event date, the additional adverse selection parameters are active. The vertical line displays the MiFID II implementation date.

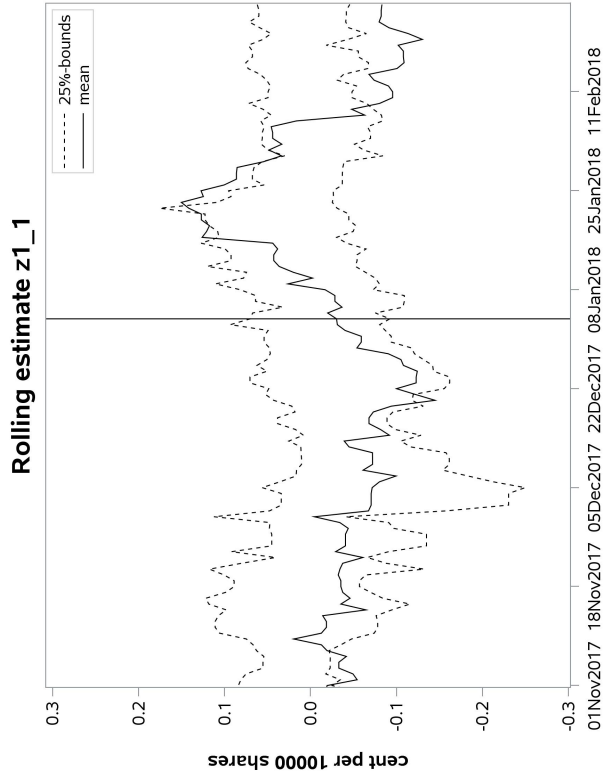


Figure 23: Rolling parameter estimate $\hat{z}_{1,1}$

Note. This figure plots the mean estimated Madhavan et al. parameter $\hat{z}_{1,1}$ per 10000 shares for event dates from November to February with a two months estimation time frame. Starting from the event date, the additional adverse selection parameters are active. The vertical line displays the MiFID II implementation date.

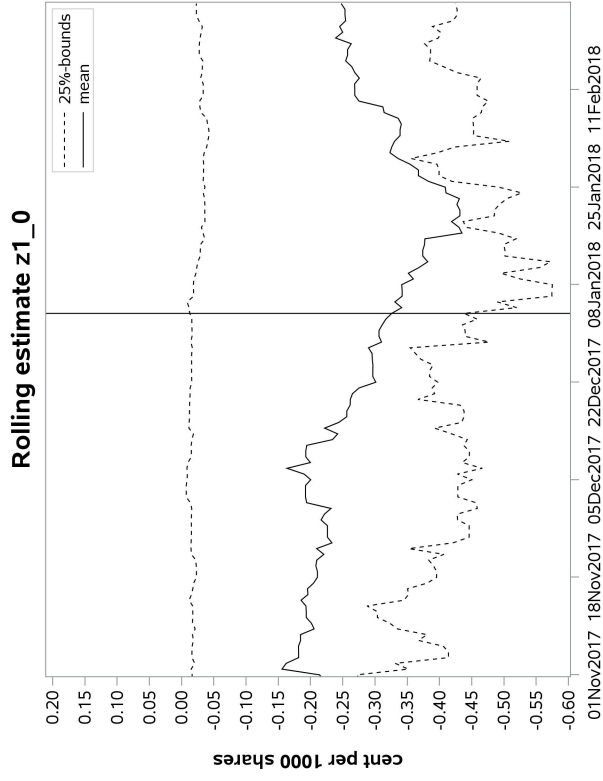


Figure 24: Rolling parameter estimate $\hat{z}_{1,0}$

Note. This figure plots the mean estimated Madhavan et al. parameter $\hat{z}_{1,0}$ per 10000 shares for event dates from November to February with a two months estimation time frame. Starting from the event date, the additional adverse selection parameters are active. The vertical line displays the MiFID II implementation date.

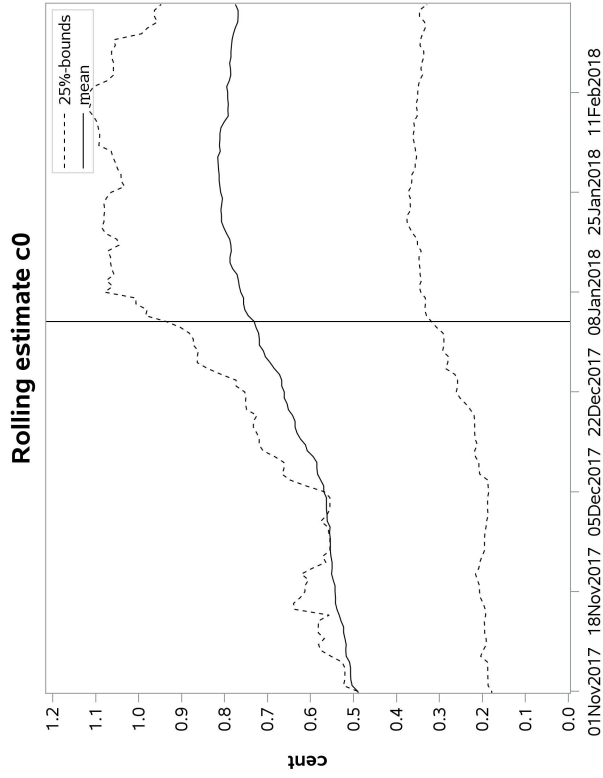


Figure 25: Rolling parameter estimate \hat{c}_0

Note. This figure plots the mean estimated Madhavan et al. parameter \hat{c}_0 for event dates from November to February with a two months estimation time frame. Starting from the event date, the additional adverse selection parameters are active. The vertical line displays the MiFID II implementation date.

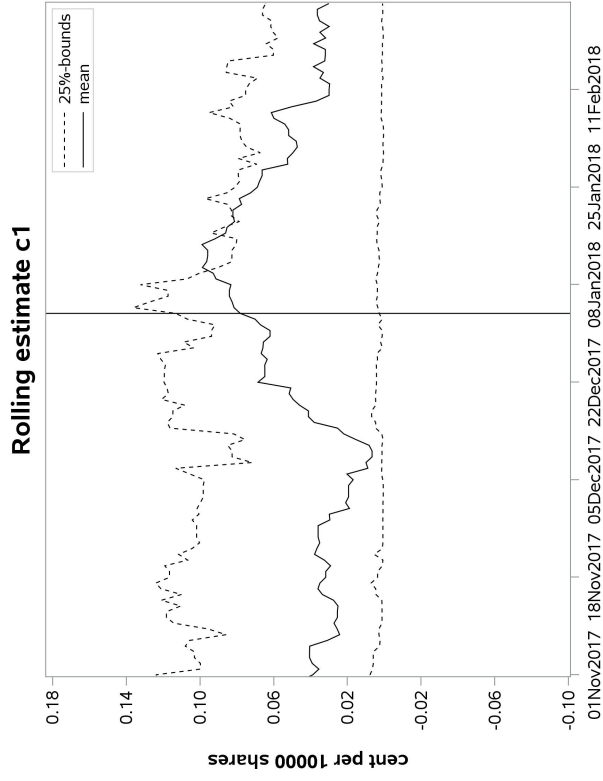


Figure 26: Rolling parameter estimate \hat{c}_1

Note. This figure plots the mean estimated Madhavan et al. parameter \hat{c}_1 per 10000 shares for event dates from November to February with a two months estimation time frame. Starting from the event date, the additional adverse selection parameters are active. The vertical line displays the MiFID II implementation date.